GEOPHYSICAL RESEARCH LETTERS, VOL. 24, NO. 24, PAGES 3177-3180, DECEMBER 15, 1997

The photochemistry of acetone in the upper troposphere: A source of odd-hydrogen radicals

S.A. McKeen,[1,2] T. Gierczak,[1,2,3] J.B. Burkholder,[1,2] P.O. Wennberg,[4] T.F. Hanisco,[4] E.R. Keim,[1,2] R.-S. Gao,[1,2] S.C. Liu,[1,5] A.R. Ravishankara,[1,6] and D.W. Fahey,[1]

Abstract. This paper summarizes measured photodissociation quantum yields for acetone in the 290-320 nm wavelength region for pressures and temperatures characteristic of the upper troposphere. Calculations combine this laboratory data with trace gas concentrations obtained during the NASA and NOAA sponsored Stratospheric Tracers of Atmospheric Transport (STRAT) field campaign, in which measurements of OH, HO_2, odd-nitrogen, and other compounds were collected over Hawaii, and west of California during fall and winter of 1995/1996. OH and HO_2 concentrations within 2 to 5 km layers just below the tropopause are ~50% larger than expected from O_3, CH_4, and H_2O chemistry alone. Although not measured during STRAT, acetone is inferred from CO measurements and acetone-CO correlations from a previous field study. These inferred acetone levels are a significant source of odd-hydrogen radicals that can explain a large part of the discrepancy in the upper troposphere. For lower altitudes, the inferred acetone makes a negligible contribution to HO_x ($HO+HO_2$), but influences NO_y partitioning. A major fraction of HO_x production by acetone is through CH_2O formation, and the HO_x discrepancy can also be explained by CH_2O levels in the 20 to 50 pptv range, regardless of the source.

Introduction

The possible importance of acetone to upper tropospheric chemistry has been a subject of inquiry for more than a decade [*Singh and Hanst*, 1981; *Chatfield et al.*, 1987]. Although the earliest reports were in the 20 to 250 pptv range [*Knop and Arnold*, 1987], more recent measurements have consistently found background levels in the 300-500 pptv range with correlative evidence for anthropogenic sources, biomass burning, and direct biogenic emissions [*Singh et al.*, 1995; *Arnold et al.*, 1997]. The sinks for atmospheric acetone are photolysis in the upper troposphere, reaction with OH in the lower troposphere and surface deposition [*Kanakidou et al.*, 1991]. Yet the budget of acetone is far from being understood. Measurements of photolysis cross-sections [e.g. *Hynes et al.*, 1992] and pressure dependent quantum yields [*Emrich and Warneck*, 1988] imply that the acetone photolysis has a significant effect on tropospheric photochemistry as a source of peroxy and alkoxy radicals, and also through the partitioning of odd-nitrogen (NO_y) between reactive (NO, NO_2) and nonreactive (PAN, HNO_3) species [*Singh et al.*, 1995]. Thus, acetone could play an important role in background O_3 formation, particularly in the upper troposphere where water vapor is typically quite low [*Wennberg et al.*, 1997].

Odd-hydrogen production from acetone photolysis begins with methyl peroxy and acetyl peroxy radical formation:

$$CH_3COCH_3 + h\nu + 2O_2 \longrightarrow CH_3O_2 + CH_3C(O)O_2 . \quad (1)$$

In the upper troposphere, NO is usually high enough for nearly all $CH_3C(O)O_2$ to be converted to CH_3O_2, which forms HO_2 through reaction with NO. An alternate photolysis channel resulting in 2 methyl radicals and CO has also been observed, but the effect of this channel on peroxy radical production is identical to (1), and is not expected to be important since its energy threshold corresponds to ~300 nm. Previous work by *Emrich and Warneck* [1988] has shown an inverse pressure dependence of the $CH_3C(O)O_2$ formation quantum yield due to an excited triplet state that is quenched by air. Our measurements, using pulsed laser photolysis, eliminates possible interferences that may have occurred in the $CH_3C(O)O_2$ yield determinations using NO_2 addition to monitor PAN formation from the NO_2 + $CH_3C(O)O_2$ reaction in the Emrich and Warneck experiments. Further, the quantity of interest is the quantum yield for dissociation of acetone and not just the formation of the acetyl radical.

The possible role of acetone is analyzed within the context of measurements collected during the STRAT campaign. The platform for these measurements was the ER-2 aircraft, and the instrument package is basically the same as in previous ER-2 field experiments [*Fahey et al.*, 1995]. OH and HO_2 measurements for STRAT are reviewed in *Wennberget al.* [1997], where upper tropospheric HO_x was consistently higher than levels expected from measured CH_4, CO, H_2O and O_3. The acetone quantum yields and cross sections are incorporated into detailed calculations, and its influence on NO_y partitioning and HO_x examined. Although the calculations are limited by steady-state assumptions, they still provide limits on the influence of acetone and indicate the extent of coupling between HO_x and NO_y chemistry.

Rate of photochemical removal of acetone

Details of the UV absorption cross section and quantum yield measurements of acetone are described in *Gierczak et al.* [1997]. Acetone UV absorption spectra were measured in a 2 m absorption cell between 215 and 350 nm over the T range 235 to 298K using a diode array spectrometer. Absorption cross sections (σ) were determined using absolute pressure measurements, and their T-dependence parameterized. The measured σ are within a few percent of those reported by *Hynes et al.* [1992] between 300-340 nm and 298-261 K, the λ and T range of overlap.

Acetone photolysis quantum yields (ϕ) were measured at 298 K using pulsed laser photolysis at 248, 266, 282, 285, 292, 301.5, 308, 321 and 337 nm in a Pyrex cell with 1 to 760 Torr of synthetic air as the buffer gas. Acetone loss was measured by gas chromatographic analysis. The 308 nm ϕ was also measured at 274, 254 and 195K, and found to vary only slightly over this range. The two parameters for the Stern-Volmer relationship between ϕ and air density were determined for λ>292 nm. Reasonable first order and log-linear fits to the parameters with λ were found, with the suggested parameterization for ϕ given in Figure 1.

[1]Aeronomy Laboratory, National Oceanic and Atmospheric Administration, Boulder, Colorado.
[2]Cooperative Institute for Research in Environmental Sciences, University of Colorado, Boulder, Colorado.
[3]Permanent address: Department of Chemistry, University of Warsaw, Warsaw, Poland.
[4]Department of Chemistry, Harvard University, Cambridge, Massachusetts.
[5]Currently at School of Earth and Atmospheric Sciences, Georgia Institute of Technology, Atlanta, Georgia.
[6]Also associated with the Department of Chemistry and Biochemistry, University of Colorado, Boulder, Colorado.

Paper number 97GL03349.
0094-8534/97/97GL-03349$05.00

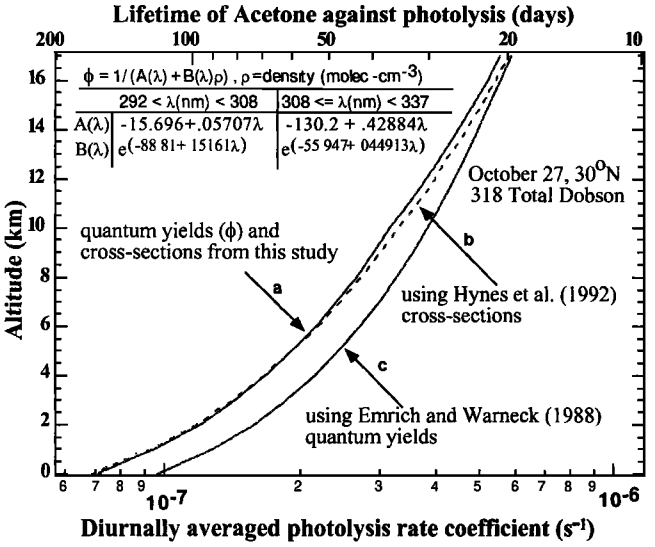

Figure 1. Diurnally averaged photolysis dissociation rate constant and lifetime for acetone for October 27, 30°N: (a) σ and ϕ from this study, (b) σ from *Hynes et al.* [1992] (model A) and ϕ from this study, (c) σ from this study and ϕ from *Emrich and Warneck* [1988]. The analytical expression for ϕ is from this study, where ρ is air density (molec.-cm^{-3}), λ is wavelength (nm).

Clear sky photolysis rate calculations are performed similar to a previous study [*McKeen et al.*, 1997]. The fit parameters for $1/\phi$ and σ are included for all λ between 295 and 345 nm. Although the slopes of $1/\phi$ are typically about 20% greater than those of *Emrich and Warneck* [1988], Figure 1 shows that the resulting ϕ at low pressures are not significantly different. At 16 km, the Emrich and Warneck ϕ result in rate constants ~8% higher than those based on this study, while at 9 km the difference is ~18%. With a 15% uncertainty assigned to ϕ and a 10% uncertainty in σ, the two studies essentially agree within the uncertainties. Below 5 km, the photolysis rate constants using ϕs from this study are ~30% less than those based on *Emrich and Warneck* [1988].

The global average of acetone's photolytic loss requires a source of 10 Tg(Carbon)/yr for every 100 pptv of acetone uniformly mixed between 0 and 17 km. Additional loss by OH reactions and surface deposition adds 40-60% [*Kanakidou et al.*, 1991; *Singh et al.*, 1995], so that a background tropospheric acetone level of 300 pptv requires sources totaling at least ~40 Tg C /yr. Direct anthropogenic emissions and formation from the oxidation of propane, C_5 and C_6 alkanes and alkenes can only account for roughly half of this source [*Singh et al.*, 1995]. Only a small fraction of the 1150 Tg C/yr biogenic emission source [*Guenther et al.*, 1995] would be necessary to balance the difference, and acetone has been observed to contribute substantially to non-methane carbon over temperate forests [e.g., *Goldan et al.*, 1995]. Given its potential importance, information regarding acetone's distribution and sources are valuable areas for research.

STRAT Observations and Model Calculations

Data from several tropospheric legs during STRAT were collected during flights near Ames, California, and Barber's Point, Hawaii, between October of 1995 and February of 1996. These level flight legs lasted 15 to 30 min., and were designed to study clear sky atmospheric composition below the tropopause. Table 1 lists the averages of several species for 13 legs determined to be in the troposphere, based on the altitude relative to the height of the minimum observed temperature. The influence of the stratosphere is evident in legs having high O_3, low CO, and low H_2O (legs 4, 8 and 11, 13-16.5 km). Legs with little stratospheric influence are noted by relatively low O_3, high CO, and high H_2O (legs 5, 9, 12 and 13, 10.5-12 km). Measurements of OH, HO_2, and the NO/NO_y ratio are used to compare with the model results.

A photochemical box model previously used to analyze clean air photochemistry [*McKeen et al.*, 1997] was applied to the conditions of STRAT. Rates, σ, and ϕ are from JPL-1994 [*DeMore et al.*, 1994] with two revisions: the $J(O^1D)\phi$ parameterization of *Michelsen et al.* [1994] and the T-dependent (250-298K) σ for PAN [*Talukdar et al.*, 1995] are used. For T <250K no extrapolation of the PAN σ are made, and 250K σ are used. Relatively low levels of C_2H_6, and sometimes C_3H_8, either detected or inferred from CO measurements, are included in the calculations; but do not significantly influence the model results. Calculated NO_2

Table 1. Averages of Species and Variables Measured During Level Flight Legs of the 1995-1996 Winter STRAT Campaign

Variable	Leg 1	Leg 2	Leg 3	Leg 4	Leg 5	Leg 6	Leg 7	Leg 8	Leg 9	Leg 10	Leg 11	Leg 12	Leg 13
Date (1995-1996)	Oct. 26	Oct. 26	Oct. 26	Oct. 26	Nov. 7	Nov. 7	Nov. 7	Nov. 7	Jan. 29	Jan. 29	Jan. 29	Feb. 2	Feb. 2
Altitude (km)	12.5	13.1	14.9	16.7	11.2	13.1	14.9	16.1	11.9	12.5	13.1	10.6	11.2
Latitude (°)	37.	37.	37.	37.	21.	21.	21.	21.	37.	37.	37.	37.	37.
Zenith Angle (°)	57.7	54.0	52.1	51.8	38.5	38.9	41.1	44.7	72.6	68.3	64.	57.4	54.2
Pressure (mb)	179.8	163.2	123.	92.4	217.9	163.4	123.1	101.4	197.7	179.6	163.0	239.4	218.
Temperature (°K)	215.4	211.9	204.4	200.9	222.2	211.	201.8	199.4	209.4	207.9	210.4	216.7	214.
O_3 (ppbv)	60.9	73.	77.1	242.5	66.4	91.7	114.6	188.6	67.9	109.7	269.1	56.6	67.4
H_2O (ppmv)	10.3	9.1	5.9	4.9	26.8	12.7	7.2	5.9	37.4	12.9	5.8	74.4	57.5
CO (ppbv)	73.3	74.1	74.9	35.5	82.	86.1	67.7	44.1	87.8	62.3	42.7	93.1	81.
NO (pptv)	128.8	145.9	213.4	262.6	122.9	208.4	192.7	205.8	108.6	100.1	82.1	35.3	83.4
NO_y (pptv)	399.1	461.3	486.2	858.3	474.2	744.7	600.8	722.3	436.3	577.3	1036.	165.7	297.7
HO_2 (pptv)	3.09	3.09	2.71	1.36	4.08	3.15	2.31	1.60	2.78	1.98	1.85	6.92	4.67
OH (pptv)	0.355	0.401	0.498	.486	0.368	0.425	0.447	0.442	0.233	0.228	0.183	0.214	0.349
Overhead O_3[a]	235.8	244.7	244.1	234.6	302.8	297.1	288.3	291.6	300.	300.	300.	367.	365.2
Surface Area[b]	1.65	2.46	2.02	1.93	2.40	5.57	4.92	2.70	2.50	2.50	2.50	1.78	2.70
--Model quantities--													
Acetone (pptv)[c]	321.	302.2	236.7	26.55	358.5	379.8	169.	77.48	1303.	474.0	265.4	1976.	1256.
HNO_3/NO_y[c]	0.607	0.611	0.513	0.635	0.673	0.65	0.565	0.585	0.556	0.664	0.782	0.347	0.580
PAN/NO_y[c]	0.082	0.073	0.045	0.006	0.084	0.064	0.039	0.02	0.218	0.113	0.08	0.495	0.224
CH_2O (pptv)[c]	18.9	17.5	14.1	5.84	25.9	21.6	11.3	7.64	25.9	13.3	9.39	34.6	28.5
CH_2O (pptv)[d]	30.1	28.7	24.2	7.1	37.6	36.2	18.1	10.8	52.6	24.6	16.5	62.6	64.1

Observed CH_4 values between 1.71 and 1.76 ppmv are also included in the analysis. H_2 is assumed to be .5 ppmv.
[a]Overhead ozone in Dobson units. The legs on January 29, 1996 are assumed to have 300 Dobsons based on the last half of the flight.
[b]Aerosol surface area is in μm^2-cm^{-3}. Values for legs on January 29, 1996 are based on the averages from all other legs.
[c]Acetone, PAN, HNO_3, and CH_2O are model derived for the case when acetone is adjusted so that model HO_x exactly matches observed HO_x.
[d]CH_2O is the fixed value necessary such that model HO_x exactly matches observed HO_x. Acetone is set to zero for this case.

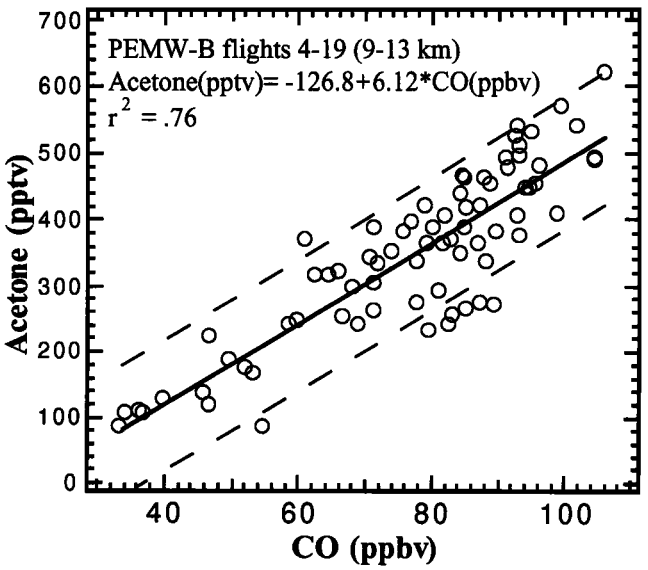

Figure 2. Correlation between acetone and CO during PEM-West(B) for all samples taken above 9 km. Dashed lines are ±100 pptv about the linear least squares regression (solid line).

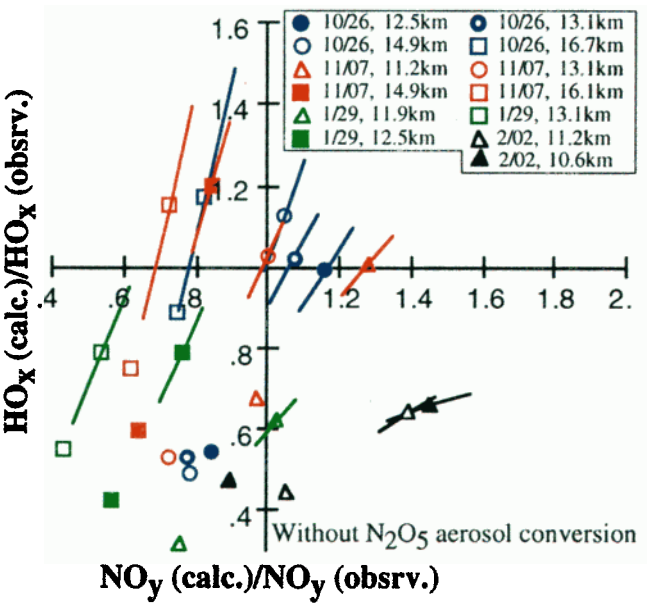

Figure 3b. Same as in Figure 3a, except N_2O_5 conversion to HNO_3 by aerosol is not included in the calculations.

and $O_3 \rightarrow O^1D$ photolysis rates compare well (within 10-15%) with measurements made during STRAT. The heterogeneous loss of N_2O_5 onto aerosol surfaces is included in the base calculations as a source of HNO_3 using the observed surface area and a reactive uptake coefficient of 0.1.

The model results represent quasi-steady-state conditions, and all of the observed variables in Table 1 are used as input. The NO_x ($NO+NO_2$), CO, O_3, CH_4, and other hydrocarbons are held constant. All others are calculated in a diurnally varying time-dependent mode until the diurnal average reaches a steady state. It is questionable whether the condition of steady state applies to the averaged air masses sampled by the ER-2, since interconversion times between NO_x, HNO_3 and PAN are on the order of a month. We can only consider the steady state assumption as a theoretical reference point in the comparison with the observations. Indeed, the comparisons for some low-altitude legs are best explained by non-steady-state conditions. The choice of constraining odd-nitrogen using observed NO rather than NO_y does not significantly influence the calculated value of NO/NO_y. *Wennberg et al.* [1997] show that the observed OH/HO_2 ratio is explained very well by the fast reactions of OH with CO, CH_4 and O_3 to form HO_2 and the return of OH by the HO_2-NO reaction. The choice of fixing NO and predicting NO_y is designed to keep model OH $/HO_2$ ratios consistent with observations.

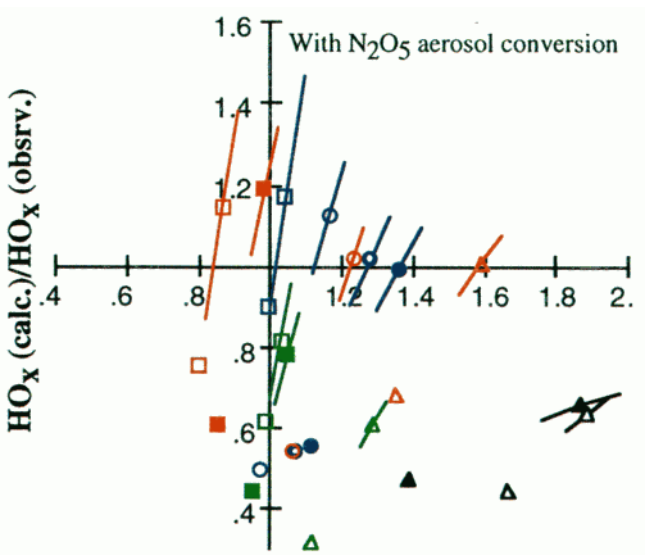

Figure 3a. Model/observed HO_x ratio versus model/observed NO_y ratio. Symbols with no line correspond to zero acetone. Symbols with lines have acetone specified by the acetone-CO regression of Figure 2, and lines correspond to the ±100 pptv acetone envelope. Squares denote legs with a strong stratospheric signal (O_3 > 100 ppbv); triangles denote legs with strong mid-tropospheric signal (H_2O > 25 ppmv); circles denote flights with neither a marked stratospheric nor mid-troposphere signal. N_2O_5 to HNO_3 aerosol conversion is included.

Acetone was not measured during STRAT, but included in the calculations by taking advantage of correlations between acetone and CO from the NASA-sponsored Pacific Exploratory Mission, Phase B (PEM-West(B)). These measurements were collected in the western Pacific between February and March of 1994 [*Singh et al.*, 1995; 1997]. Figure 2 shows upper tropospheric acetone versus CO for PEM-West(B). Nearly all acetone values fall within ±100 pptv of the linear regression line. CO from STRAT is combined with the regression in Figure 2 to define acetone for the calculations. The good correlation shown in Figure 2 is related to the tight inverse correlations between CO and O_3, and acetone and O_3, observed in PEM-West(B) [*Singh et al.*, 1997], which are explained in terms of bulk compositional differences between the stratosphere and troposphere. By inference this is also the reason for the acetone-CO correlation. The regression slope may depend on season and location since tropospheric sources may not be coincident.

Model Results and Conclusions

Figure 3a shows predicted/observed ratios of HO_x and NO_y when the CO-acetone correlation and the ±100 pptv envelope of Figure 2 are included in the calculations. Without additional radical sources, all calculations below 16.5 km underpredict HO_x by 25% to 60%, well outside the uncertainty limits of the measurements [*Wennberg et al.*, 1997]. Except for the three low-altitude legs 9, 12, and 13, the addition of expected acetone levels causes HO_x to straddle or fall within 12% of the observations. Within the uncertainties of the CO correlation, acetone appears to

be a significant source of upper-tropospheric HO_x, and provides the amount of HO_x necessary to explain the difference between observed HO_x and calculations based only on O_3, H_2O and CH_4.

The abscissa of Figure 3a measures the model's ability to predict NO/NO_y ratios. Many of the low-altitude legs overpredict NO_y with no acetone, and increase NO_y further with its addition. However, NO_y for the higher-altitude legs are within 20% of the observations. Model NO_y is sensitive to assumptions influencing HNO_3-NO_x partitioning, as illustrated by the differences in Figures 3a and 3b. Figure 3b is similar to Figure 3a, except N_2O_5 aerosol conversion to HNO_3 is absent. Flight legs with strong stratospheric characteristics underpredict NO_y without N_2O_5 conversion, similar to previous stratospheric results [*Fahey et al.*, 1993]. NO_y predictions for flight legs at lower altitudes in Figure 3b show much better agreement, suggesting that the model would match the observations if the reactive uptake coefficient for conversion of N_2O_5 was much less than 0.1. This could be the case if sulfate in the tropospheric aerosol were neutralized, say to ammonium sulfate, which has a factor of 10 smaller N_2O_5 uptake coefficient compared to sulfuric acid droplets for low relative humidities [*Hu and Abbat*, 1997]. Previous explanations of high NO_x/NO_y ratios have invoked a missing HNO_3 to NO_x conversion process [e.g. *Chatfield*, 1994]. Episodic processes such as NO_x injection by lightning or convection, or removal of HNO_3 by clouds could also explain the NO_y discrepancies in Figure 3a. The slopes of the traces in Figures 3a,b show the coupling between odd-hydrogen and odd-nitrogen with acetone additions. This is largely due to the conversion of NO_x to HNO_3 by OH. The reduced slopes for the low altitude legs are the result of a decreased HO_x sensitivity to acetone from higher H_2O levels, and increases of PAN relative to NO_x from lower PAN photolysis rates.

The last four rows of Table 1 illustrate the NO_y partitioning and radical chemistry when HO_x sources are adjusted to force calculated HO_x to the observations. If acetone is the forcing agent, PAN/NO_y ratios are still reasonably low for all but the lowest altitudes, and in good agreement with previous PAN/NO_y measurements between 7 and 12 km over the Pacific [*Singh et al.*, 1996]. For the four legs with PAN/NO_y ratios >0.1, the acetone needed is greater than indicated by the CO-acetone relationship. However, the PAN/NO_y ratios for T < 230 K are sensitive to the treatment of PAN absorption σ. If the T-dependence within *Talukdar et al.* [1995] is extrapolated to 200 K, PAN increases ~50%.

In general, the acetone levels expected from the CO measurements account for a majority of the missing HO_x when $[H_2O]$ < 25 to 30 ppmv. Sources other than acetone are required to explain observed HO_x at lower altitudes [*Jaeglé et al.*, this issue]. The last two rows in Table 1 compare the CH_2O from acetone additions to the case where only CH_2O is adjusted to force HO_x to observed levels. The CH_2O formed from acetone accounts for 50% to 85% of the source necessary to match the HO_x observations, yet these levels are quite low compared to the sensitivity of existing measurement techniques. In order to understand upper tropospheric HO_x sources, acetone and accurate CH_2O measurements should be made in conjunction with HO_x.

Acknowledgements. This research was supported in part by the Atmospheric Chemistry Project of the Climate and Global Change Program of NOAA, as well as the Upper Atmospheric Research and Atmospheric Effects of Aviation Projects within NASA. We are indebted to the pilots, crew and mission scientists of the STRAT campaign. They include E. Atlas, J. Margitan, M. H. Proffitt, E. Hintsa, T. E. McElroy, J. Wilson, C. R. Webster, R. D. May, R. Herman, and K. R. Chan. Discussions with Ross Salawitch, Lyatt Jaeglé, Daniel Jacobs, Robert Chatfield, Hanwant Singh, and Michael Trainer are also greatly appreciated.

References

Arnold, F., J. Schneider, K. Gollinger, H. Schlager, P. Schulte, D. E. Hage, P. D. Whitefield, and P. van Velthoven, Observation of upper tropospheric sulfur dioxide- and acetone-pollution: Potential implications for hydroxyl radical and aerosol formation, *Geophys. Res. Lett.*, 24, 57-60, 1997.

Chatfield, R. B., E. P. Gardner, and J. G. Calvert, Sources and sinks of acetone in the atmosphere: Behavior of reactive hydrocarbons and a stable product, *J. Geophys. Res.*, 92, 4208-4216, 1987.

Chatfield, R. B., Anomolous HNO_3/NOx ratio of remote tropospheric air: Conversion of nitric acid to formic acid and NOx? *Geophys. Res. Lett.*, 21, 2705-2708, 1994.

DeMore, W. B., M. J. Molina, S. P. Sander, D. M. Golden, R. F. Hampson, M. J. Kurylo, C. J. Howard, and A. R. Ravishankara, Chemical kinetics and photochemical data for use in stratospheric modeling, *Evaluation number 10, JPL Pub. 94-26*, 1994.

Emrich, M., and P. Warneck, Photodecomposition of acetone, in Mechanisms of gas phase and liquid phase chemical transformations in tropospheric chemistry, EUR 12035, edited by R.A. Cox, pp. 29-32, Brussels, 1988.

Fahey, D.W., et. al., In situ measurements constraining the role of sulphate aerosols in mid-latitude ozone depletion, *Nature*, 363, 509-514, 1993.

Fahey, D. W., et al., In situ observations in exhaust plumes in the lower stratosphere at midlatitudes, *J. Geophys. Res.*, 100, 3065-3074, 1995.

Gierczak, T., J. B. Burkholder, S. Bauerle, and A. R. Ravishankara, Photochemistry of acetone under tropospheric conditions, submitted to *Chem. Phys.*, special issue honoring I. Tanaka, 1997.

Goldan, P. D., W. C. Kuster, F. C. Fehsenfeld, and S. A. Montzka, Hydrocarbon measurements in the southeastern United States: The Rural Oxidants in the Southern Environment (ROSE) Program 1990, *J. Geophys. Res.*, 100, 25,945-25,963, 1995.

Guenther, A., et al., A global model of natural volatile organic compound emissions, *J. Geophys. Res.*, 100, 8873-8892, 1995.

Hu, J. H., and J. P. D. Abbat, Reaction probabilities for N_2O_5 hydrolysis on sulfuric acid and ammonium sulfate aerosols at room temperature, *J. Phys. Chem.*, 101, 871-878, 1997.

Hynes, A. J., E. A. Kenyon, A. J. Pounds, and P. H. Wine, Temperature dependent cross-sections for acetone and n-butanone - implications for atmospheric lifetimes, *Spectrochimica Acta*, 48A, 1235-1242, 1992.

Jaeglé, L., et al., Influence of convection on upper tropospheric OH and HO_2, submitted to *Geophys. Res. Lett.*, this issue, 1997.

Kanakidou, M., H. B. Singh, K. M. Valentin, and P. J. Crutzen, A two-dimensional model study of ethane and propane oxidation in the troposphere, *J. Geophys. Res.*, *96*, 15,395-15,413, 1991.

Knop, G., and F. Arnold, Stratospheric trace gas detection using a new balloon-borne ACIMS method: Acetonitrile, acetone, and nitric acid, *Geophys. Res. Lett.*, 14, 1262-1265, 1987.

McKeen, S.A., et al., Photochemical modeling of hydroxyl and its relationship to other species during the tropospheric OH photochemistry experiment, *J. Geophys. Res.*, *102*, 6467-6494, 1997.

Michelsen, H.A., R. J. Salawitch, P.O. Wennberg, and J. G. Anderson, Production of $O(^1D)$ from photolysis of O_3, *Geophys. Res. Lett.*, 21, 2227-2230, 1994.

Singh, H. B., and P. L. Hanst, Peroxyacetyl nitrate (PAN) in the unpolluted atmosphere: An important reservoir for nitrogen oxides, *Geophys. Res. Lett.*, *8*, 941-944, 1981.

Singh, H. B., M. Kanakidou, P. J. Crutzen, and D. J. Jacob, High concentrations and photochemical fate of oxygenated hydrocarbons in the global troposphere, *Nature*, *378*, 50-54, 1995.

Singh, H. B., et al., Reactive nitrogen and ozone over the western Pacific: Distribution, and sources, *J. Geophys. Res.*, *101*, 1793-1808, 1996.

Singh, H. B., et al., Trace chemical measurements from the northern midlatitude lowermost stratosphere in early spring: Distributions, correlations, and fate, *Geophys. Res. Lett.*, *24*, 127-131, 1997.

Talukdar, R. K., J. B. Burkholder, A.-M. Schmoltner, J. M. Roberts, R. R. Wilson, and A. R. Ravishankara, Investigation of the loss processes for peroxyacetyl nitrate in the atmosphere: UV photolysis and reaction with OH, *J. Geophys. Res.*, *100*, 14163-14174, 1995.

Wennberg, P., et al., Hydrogen radicals, nitrogen radicals, and the production of ozone in the middle and upper troposphere, submitted to *Science*, 1997.

J.B. Burkholder, D.W. Fahey, R.-S. Gao, T. Gierczak, E.R. Keim, S.A. McKeen, A.R. Ravishankara, NOAA/ERL, 325 Broadway, Boulder, CO 80303-3328. (e-mail: stu@al.noaa.gov)

T.F. Hanisco, and P.O. Wennberg, Department of Chemistry, Harvard Univeristy, 12 Oxford St., Cambridge, MA 01238.

S.C. Liu, School of Earth and Atmospheric Sciences, Georgia Tech, Atlanta GA 30350.

(Received May 8, 1997; revised October 30, 1997;
accepted November 11, 1997)